Geotextiles and Geomembranes. Submitted 13 November 2016; accepted 2 July 2017.
http://dx.doi.org/10.1016/j.geotexmem.2017.07.004

Creep analysis of an earth embankment on soft soil deposit with and without PVD improvement

Mohammad Rezania[a,*,1], Meghdad Bagheri[b,2], Mohaddeseh Mousavi Nezhad[a,3], Nallathamby Sivasithamparam[c,4]

[a]School of Engineering, The University of Warwick, Coventry CV4 7AL, UK

[b]Department of Civil Engineering, The University of Nottingham, Nottingham NG7 2RD, UK

[c]Computational Geomechanics Division, Norwegian Geotechnical Institute, Oslo No-0806, Norway

Abstract

In this paper, an anisotropic creep constitutive model, namely Creep-SCLAY1S is employed to study the installation effects of prefabricated vertical drains (PVDs) on the behavior of a full scale test embankment, namely Haarajoki embankment in Finland. The embankment was constructed on a natural soft soil with PVD installed to improve the drainage under one half of it. The Creep constitutive model used in this study, incorporates the effects of fabric anisotropy, structure and time within a critical state based framework. For comparison, the isotropic modified Cam clay (MCC) model and the rate-independent anisotropic S-CLAY1S model are also used for the analyses. The numerical predictions are compared with field measurements and the results indicate that the creep model provides an improved approximation of field settlements, and excess pore pressure build-up and dissipations. In addition, the application of two commonly used permeability matching techniques for two dimensional (2D) plane-strain analysis of the PVD problem is studied and the results are discussed highlighting their limitations and advantages.

*,[1]Corresponding author. E-mail address: m.rezania@warwick.ac.uk. Tel.: +44 24 76 522339.

[2] E-mail address: meghdad.bagheri@nottingham.ac.uk. Tel.: +44 115 95 12850.

[3] E-mail address: m.mousavi-nezhad@warwick.ac.uk. Tel.: +44 24 765 22332.

[4] E-mail address: nallathamby.siva@ngi.no. Tel.: +47 406 94 933.

Geotextiles and Geomembranes. Submitted 13 November 2016; accepted 2 July 2017.
http://dx.doi.org/10.1016/j.geotexmem.2017.07.004

Keywords: Geosynthetics; Embankment; PVD; Soft clay; Creep behavior; Advanced constitutive model

1 Introduction

In order to tackle the delayed consolidation settlement problem typical of soft soils, installation of prefabricated vertical drains (PVDs), combined with preloading, has become popular in the industry as an effective ground improvement solution (e.g. Abuel-Naga et al. 2015, Lam et al. 2015, Wang et al. 2016). Preloading is an old way of dealing with the problem of long-term consolidation in soft soils; however, in practice, this procedure on its own can be considerably time consuming. For the excess pore water pressure (PWP) to be dissipated quickly, the drainage paths need to be shortened. PVDs are geosynthetic slender elements made of corrugated plastic cores that their installation can effectively reduce the consolidation time as they provide short horizontal drainage paths in thick soft soil deposits that need improvement (Rowe and Taechakumthorn 2008).

Some aspects of PVD installation e.g., well resistance, smear effect and the overlapping of smear zones have been widely studied (e.g. Kim and Lee 1997, Zhu and Yin 2000, Cascone and Biondi 2013, Deng et al. 2013, Xue et al. 2014, Chen et al. 2016, Nguyen and Indraratna 2017). However, very few studies exist regarding the long-term effects of PVD installation on the response of the soft soil layer (e.g. Kim 2012, Lo et al. 2013, Hu et al. 2014), this deemed to be in part due to the unavailability of appropriate soil models. Many soil constitutive models, which are commonly used for the analysis and design of geotechnical engineering problems, assume that the behavior of soil is simply isotropic. Application of such simplified models in practice often provide solutions that are overly conservative and costly, and in some cases result in uncertainties regarding long-term performances. In reality, the behavior of natural soils is highly anisotropic. Natural clays also have an inherent structural property that gives them an undisturbed shear strength in excess of their remolded strength. Furthermore, clayey soils are known to be the most susceptible to time effects on their strength and deformation characteristics. An accurate prediction of soft soil response, either improved or unimproved,

requires that these aspects of their behavior are considered by the employed constitutive model.

Because of considerable computational cost of three dimensional (3D) finite element (FE) analysis, the boundary value problems related to PVD ground improvement are commonly modeled in the representative 2D plane-strain condition. As water flow into the PVD is an axisymmetric problem; therefore, for the representative 2D analysis, a number of so-called mathematical matching techniques have been proposed (e.g. Hird et al. 1992, Lin et al. 2000, Indraratna et al. 2005). These matching methods are used for the conversion of permeability coefficient from axisymmetric state into plane-strain condition.

The focus of this paper is, to assess the long-term behavior of an embankment on soft clay deposit with and without PVD improvement, and to examine the applicability of a recently developed creep constitutive model in predicting ground deformations at a practical level. For this study, Haarajoki test embankment (Finish National Road Administration, 1997) is numerically simulated using an advanced creep constitutive model, namely Creep-SCLAY1S (Sivasithamparam et al. 2015). This test embankment is constructed on deep soft soil deposit improved with PVDs for one half of its length. The results from the newly developed creep model are compared with those obtained by using a time-independent anisotropic model, S-CLAY1S (Karstunen et al. 2005), and the MCC model (Roscoe and Burland, 1968). In addition, a simple comparative study is carried out in order to examine the sensitivity of the results to the adopted matching technique.

2 Creep-SCLAY1S Model

The Creep-SCLAY1 (Sivasithamparam et al. 2015) is an extension of S-CLAY1 (Wheeler et al. 2003) to incorporate rate-dependent response of clays. In this model the elliptical surface of the S-CLAY1 model is adopted as the Normal Consolidation Surface (NCS), i.e. the boundary between small and large irreversible (creep) strains; furthermore, creep is formulated using the concept of a constant rate of visco-plastic multiplier (Grimstad et al.

2010). The new creep model incorporates the same rotational hardening law as that of the S-CLAY1 and S-CLAY1S models. Moreover, the Creep-SCLAY1 model has been further extended by incorporating the destructuration hardening law of the S-CLAY1S model to take into account the effect of the initial inter-particle bonding in the soil response. Despite assuming anisotropy of plastic behavior, the S-CLAY1 class of models assume isotropy of elastic behavior which is a reasonable assumption for modeling the behavior of soft and sensitive clays (Rezania et al. 2016). In addition to the soil parameters required for modeling with SCLAY1S (as detailed in Karstunen et al. 2005), the use of Creep-SCLAY1S requires three viscous parameters namely, the reference time, τ, the modified creep index, μ^*, and the intrinsic value of the modified creep index, μ_i^*. Note that μ^* is related to the one-dimensional secondary compression index, C_α, as

$$\mu^* = C_\alpha/[\ln 10\ (1 + e_0)] \quad (1)$$

The extended Creep-SCLAY1S model has recently been successfully applied for modeling pile installation effects in a soft clay deposit (Rezania et al. 2017).

3 Numerical modeling of PVD improved ground

For planning a PVD ground improvement work, penetration depth, installation pattern and spacing of PVDs are the important factors that need to be taken into consideration. For the Haarajoki embankment the length of the PVDs used was 15 m and for simplicity they were installed in a square pattern (Fig. 1a) with spacing, $S = 1\ m$ and equivalent diameter, $D = 1.13\ m$. For modeling purposes, the diameter of installation induced smear zone, D_s (see Fig. 1b), is often considered to be in the range of 3-5 times the diameter of the mandrel, D_m, or 5-8 times the equivalent drain diameter, D_w (Xiao 2001).

Ideally the study of PVD ground improvement is a 3D problem, requiring a 3D FE analysis. This is due to the fact that the seepage and consolidation around vertical drains are in reality 3D. However, such a model would be computationally very expensive and time consuming,

Geotextiles and Geomembranes. Submitted 13 November 2016; accepted 2 July 2017.
http://dx.doi.org/10.1016/j.geotexmem.2017.07.004

mainly due to the need for discretely modeling each vertical drain and its associated influence zone (Yildiz 2009) that can result in mesh complexity and therefore increased convergence time and required computer memory. Therefore, often a 2D plane-strain FE model is used and a matching technique is employed to convert the general permeability of the medium into an equivalent plane-strain value. In practice, the axisymmetric unit cell representing a drain is simplified into a plane-strain unit cell, assuming an equivalent half width, B, for the cell.

A number of simplified matching approaches are available in the literature which are based on manipulation of, either the drain spacing or the soil permeability. For the simplicity of relationships each drain is assumed to work independently, a constant soil permeability is adopted and consolidation is considered to take place in a uniform soil column with linear compressibility characteristics (Yildiz et al. 2009). Comparing the numerical results in literature, it seems that the 2D plane-strain analyses do not give a satisfactory agreement in estimating the maximum value of excess pore pressure after construction (e.g. Yildiz et al. 2009). This may be because the geometry and/or the permeability of the domain are changed but the compressibility of the soil itself remains constant. Nonetheless, regardless of this issue, the matching technique proposed by Hird et al. (1992) appears to be the most convenient one as it allows the mesh size to be controlled. Another advantage of this technique is that no particular smear zone is required to be considered in the modeling.

A simple permeability matching technique has also been proposed by Lin et al. (2000), where matching is done for the horizontal permeability (see Equation (2))

$$k_{hpl} = \frac{k_h \pi}{6\left[\ln\left(\frac{n}{s}\right) + \frac{k_h}{k_s}\ln(s) - \frac{3}{4}\right]} \tag{2}$$

where k_{hpl} is the equivalent horizontal permeability of surrounding soil in plane-strain condition, k_h is the horizontal permeability of the undisturbed soil, k_s is the horizontal permeability of the smeared zone, $n = R/R_w$ and $s = R_s/R_w$ where R, R_w and R_s are the radiuses of the unit cell (equivalent radius), the drain, and the smear zone, respectively. In this

paper the matching technique proposed by Hird et al. (1992), and the one proposed by Lin et al. (2000) have been used to carry out the numerical analyses.

The drain adopted at the site was reported to have an average width of 98.7 mm with a discharge capacity of 157 m^3/year. The equivalent diameter of the drain, calculated according to the formulation proposed by Hansbo (1979) is 67 mm. Considering for the smear effect the ratios $k_h/k_s = 20$ and $D_s/D_w = 8$, values that proved to give accurate results when used with the advanced constitutive models of the S-CLAY family (Yildiz et al. 2009); the equivalent plane-strain permeability is $k_{hpl} = 0.0126k_h$.

The advanced models, S-CLAY1S and Creep-SCLAY1S, have been implemented into the finite-element code PLAXIS AE (Brinkgreve et al. 2014) through the user-defined soil model facility of the software (Rezania et al. 2014). Details of the simulations carried out, and the analysis of the results, in comparison with field measurements, are discussed in the following.

3.1 Haarajoki embankment

Haarajoki embankment has a height of 2.9 m and a length of 100 m. Its crest is 8 m wide and the slopes have a gradient of 1:2. It was founded on a 2 m thick dry crust lying above a 20.2 m thick soft clay deposit. The foundation soil consists of soft soil with a high degree of anisotropy and some inter-particle bonding. Half of the embankment (50 m long section) was constructed on PVD improved soft soil and the other half was built on the natural soft soil without any ground improvement measure.

A finite element mesh with 6-noded triangular elements is used for the FE analyses, with extra degrees of freedom for excess PWP at corner nodes (during consolidation analysis). Mesh sensitivity studies have been done to ensure that the mesh is dense enough to produce accurate results. The geometry of the FE model is shown in Fig. 2; for the model, the far right boundary is assumed at 40 m distance from the centerline. The bottom boundary of the clay deposit is assumed to be completely fixed in both horizontal and vertical directions; whereas, the left and right vertical boundaries are only restrained horizontally. Drainage is allowed at

the ground level, while due to unknown hydraulic conditions at the bottom boundary, this boundary is considered impermeable. Impermeable drainage boundaries are also assigned to the lateral boundaries. Based on ground data, the water table is assumed to be at the ground surface. For the side of the embankment that was built on improved soil, PVDs are incorporated in the model using the drain element in PLAXIS. Groundwater head is assumed to be at ground level for all drains.

The embankment was built in 0.5 m thick layers and each layer was placed and compacted within 2 days, except for the foundation layer which was built within 5 days. For the calculation phases, plastic analyses are carried out corresponding to the construction process of the embankment, after which the consolidation analysis is performed.

3.1.1 Parameters estimation

For the numerical simulation, the embankment itself is modeled using the simple linear elastic-perfectly plastic Mohr-Coulomb model with the following reported values for the embankment material: Young modulus E = 40000 kPa, Poisson's coefficient ν = 0.35, cohesion c' = 2 kPa, friction angle ϕ' = 40°, unit weight γ = 21 kN/m^3. The first layer (0-2 m) of the underlying deposit is divided into two parts; the first sub-layer (0-1 m) is modeled with the Mohr-Coulomb model using E = 2300 kPa, c' = 1 kPa and ϕ' = 30°. The second sub-layer (1-2 m) is modeled by assigning the relative advanced soil constitutive model used in the analysis without consideration of the effect of soil structure, given that the soil at this layer has low sensitivity due to being fairly disturbed. The values of model constants and state variables used for different soil layers, as reported by Karstunen et al. (2015), are summarized in Table 1.

Variation of permeability k with void ratio e during consolidation analysis is represented in simulations through permeability change index parameter c_k which is calculated according to the following equation proposed by Berry and Poskitt (1972)

$$c_k = \frac{e - e_0}{\log\left(\frac{k}{k_0}\right)} \tag{3}$$

Geotextiles and Geomembranes. Submitted 13 November 2016; accepted 2 July 2017.
http://dx.doi.org/10.1016/j.geotexmem.2017.07.004

The c_k values can be obtained from the results of oedometer tests. The same test results can be used to determine the value of creep index, C_α, and subsequently creep parameter, μ_i^*, (Sivasithamparam et al. 2015). According to Mesri and Godlewski (1977), the ratio of C_α/λ can be considered to be constant for each clay layer. The intrinsic value of the creep index $C_{\alpha i}$ (the subscript i stands for the intrinsic values) corresponding to the intrinsic compression index λ_i of each layer can be obtained from $C_\alpha \lambda_i/\lambda$. The values of μ_i^* are essentially derived using Equation (1). It should be noted that the values of μ_i^* significantly influences the results; therefore, its appropriate calibration is essential for realistic modeling of the long-term soil behavior. For determination of μ_i^* values based on the abovementioned approach, a number of available laboratory test data were carefully interpreted and the C_α and λ values which provide best simulation results were selected. Finally, the values of modified intrinsic compression and swelling indexes, λ_i^* and κ^*, are obtained as $\lambda_i^*= \lambda_i/(1+e)$ and $\kappa^*= \kappa/(1+e)$ with *e* being the void ratio (Leoni et al., 2008). Furthermore, Table 2 summarizes the parameter values used for the calculation of the equivalent plane-strain permeability, according to the employed matching technique. The modified coefficients of permeability, k_{hpl}, for the soil layers are presented in Table 3.

3.1.2 Results and discussion

3.1.2.1 Settlements

Fig. 3a shows settlement predictions versus time at the node directly under the centerline of the embankment (point A in Fig. 2) for the side of the embankment that is not improved with PVDs. It can be seen in the figure that the creep model provides an improved prediction of the field measurements, however it is clearly on the conservative side. MCC grossly underestimates the settlements. It is capable to accurately predict the settlement that occurred in early stages; however, the predicted settlement rate slows down after about day 50, pointing out that the model cannot take into consideration the time-dependent aspect of the soil behavior. Application of S-CLAY1S model leads to a similar settlement prediction trend, but,

compared to MCC, it provides a less conservative modeling result as it considers the effects of inherent features of natural soil behavior, particularly destructuration (i.e., strain softening).

Vertical settlement plots calculated for the side of the embankment built on the PVD improved soil are presented in Fig. 3b. It is observed that all three constitutive models capture the effect of PVD installation on accelerating the settlement of the soft ground. Settlement prediction by Creep-SCLAY1S model matches well with the field observations. It demonstrates that the model is capable of providing an enhanced simulation for complex scenarios where soil strata consists of both undisturbed and disturbed (smear zone) segments combined with drainage elements.

Surface settlement field data is available for the side of the embankment that was built on unimproved soil. The measurements were taken on 10 days, 5 years and 10.7 years after construction. The data has been used to investigate the surface settlement through predictions from different models (see Fig. 4). With regards to the embankment side that was built on the unimproved ground (Fig. 4a), all numerical simulations show limited vertical settlements outside the embankment area; however, Creep-SCLAY1S predicts more surface heaving in this area, particularly in short-term. All three models provide good estimation of the surface settlements shortly after construction (i.e., after 10 days). However, in long-term, MCC model grossly underestimates the surface settlements; while S-CLAY1S provides an improved prediction, although still underestimating the field data. The Creep-SCLAY1S model is able to significantly better capture the field observations, while still underestimating the vertical displacements after 5 and 10 years.

The numerical simulation results for the effect of PVD installation on the surface settlements, up to a distance of 40 m from the centerline of the embankment, can be observed in Fig. 4b. No field data is available for this side of the embankment; hence, the simulation results are presented for the same times when measurements were taken for the other half of the embankment. For all of the soil models, the predicted trends are almost the same as the case

without PVDs (see Fig. 4b). The predicted vertical settlement immediately after construction remains very similar to the unimproved side of the embankment; however, for the longer time periods the increased amounts of vertical settlements are apparent, in particular for when the advanced models S-CLAY1S and Creep-SCLAY1S are used.

Estimation of the settlement influence zone is particularly important for planning the construction work in urban areas with dense concentrations of buildings. The span of settlement influence zone predicted by different models is different. For both sides of the embankment the Creep-SCLAY1S model predicts a large influence zone (e.g., about 30 m from the centerline of the embankment on the unimproved side), whereas MCC and S-CLAY1S models clearly predict a smaller influence zone (e.g., up to about 16 m on the unimproved side). From the figure, the extent of the influence zone seemingly decreases on the side where the vertical drains are installed (see Fig. 4b), for example on this side MCC and SCLAY1S predict an influence zone of less than 10 m and Creep-SCLAY1S predicts an influence zone of less than 30 m.

3.1.2.2 Lateral displacements

For the unimproved side of the embankment, the lateral displacement predictions underneath the crest (4 m from the centerline) of the embankment after 15 days, 1 year and 3 years of consolidation, are presented in Fig. 5a and are compared with the field data. From the results, MCC and S-CLAY1S evidently underestimate the lateral displacements of the soft soil deposit, particularly at higher ground levels. Creep-SCLAY1S is able to accurately predict the maximum value of lateral displacement under the crest; however, for deeper ground levels it overestimates the deformations. This could be partly due to the approximating approach used for the determination of the creep index. All three models are able to predict the depth at which the maximum horizontal displacement occurs (2.5 m), with Creep-SCLAY1S providing more representative predictions.

For the PVD improved side of the embankment, except for the top ground layer, all three models provide reasonably good prediction of the lateral displacements under the

embankment crest in short-term (after 15 days consolidation) (Fig. 5b). The relatively large displacement at the field near the ground surface is believed to be caused by error in the field measurements. According to the field data, by comparing the measurements on both sides of the embankment it appears that the installation of PVDs does not result in significant differences on the amount of lateral displacements in short-term.

For the horizontal displacements at the toe of the embankment, generally all three models provide reasonable predictions for the side of the embankment that is built on the unimproved foundation soil (Fig. 6a). Overall, MCC and S-CLAY1S models underestimate the lateral displacements at shallow depths, while Creep-SCLAY1S overestimates the horizontal displacements a year after construction but provides more accurate predictions of lateral displacements 3 years after construction. Better approximations of the lateral deformations at deeper depths are obtained from the MCC and SCLAY1S models, while Creep-SCLAY1S overestimates the lateral deformations at these depths.

With regards to the part of the embankment that is built on the PVD improved ground, all three models fairly overestimate the amount of lateral displacements under the embankment toe after 3 years of consolidation (Fig. 6b). This could be due to the fact that friction effects between the soft soil and the PVDs are neglected in the numerical simulations. The narrowly spaced PVDs are believed to act as some sort of “reinforcements” that can reduce the long-term lateral displacements.

3.1.2.3 Excess pore pressure

Pneumatic piezometers were installed at different depths underneath the embankment to monitor the excess PWP variations with time. Measurements are available only for the half of the embankment built on the unimproved ground; however, the numerical simulation results of the PWP dissipation are obtained for both sides of the embankment. Fig. 7a shows the *in-situ* measurements of PWP related to piezometers located at a depth of 4 m, 7 m, 10 m, and 15 m under the centerline. The actual pore pressure measurements are rather erratic, not following a regular trend, particularly for the depth of 4 m, therefore the field data should not

be assumed as definitive. The excess PWP initially builds up during the embankment construction and then it is gradually dissipated with time. It is seen in Fig. 7a that all three constitutive models overestimate the initial excess PWP build-up at 4 m and 7 m depths. However, a relatively accurate prediction of initial excess PWP is obtained at deeper depths i.e. 10 m and 15 m.

Considering the plots of PWP dissipation with time in Fig. 7a, it is observed that the dissipation rate is faster when the isotropic MCC and time-independent SCLAY1S models are used, while the application of the Creep-SCLAY1S results in the slowest rate of excess PWP dissipation. This trend is observed at all depths analyzed here. Note that at 10 m and 15 m depths, the predictions of Creep-SCLAY1S show an increasing build-up of excess PWP up to day 650 (not shown here) from when the dissipation of excess PWP is commenced.

For the embankment side that was built on the PVD improved ground, all three models initially show a sharp increase in the amount of excess PWP immediately after construction, followed by a faster dissipation rate which is sensible as additional dissipation paths are provided by the PVDs to discharge excess pore pressures (Fig. 7b). The results in Fig. 7 are presented for the first 500 days of consolidation; however, the numerical analysis showed that when the MCC model is used the excess PWP fully dissipated after 3500 days of consolidation, this is the time that according to MCC consolidation settlement stops progressing. When S-CLAY1S and Creep-SCLAY1S models are used the PWP dissipation prolongs into the following years which is why with these models the consolidation settlement is continually progressing.

3.1.2.4 Stress field and state parameters

The installation of vertical drains also alters the stress field underneath the embankment. The presence of drains leads to an increase in the mean effective stress values in the region near the drains, while far from the drains the mean effective stress values approximately return to that of the field underneath the embankment side without PVDs. Fig. 8a shows the mean effective stress distribution along the embankment foundation 15 days after construction and at a depth of 2.7 m, using the Creep-SCLAY1S model. The same behavior, but with lower

peaks at the drain locations, is observed for when several years of consolidation have passed. Note that, due to the close spacing of PVDs, directly underneath the embankment the mean effective stress values are continually increasing and decreasing.

Along with the stress field, column installation also influences the state parameters of the soil such as void ratio. Void ratio decreases near the drains (see Fig. 8b) indicating a densification of the soil due to fast drainage in this area. In between the drains, the value of the void ratio increases, but it does not reach the values corresponding to when the foundation soft soil is unimproved.

In a similar manner, the presence of PVDs influences the structure of the soil. Considering destructuration parameter χ (Fig. 8c), the presence of drains causes a decrease of this state parameter at the proximity of the drains, which is likely to be due to the disturbance caused by the presence of the drain. The recovery in between the drains does not reach the values of the simulation without PVDs.

3.2 Matching techniques

As discussed earlier, different matching techniques can be adopted to calculate the equivalent permeability for the soil deposit when PVDs are installed. In this study the applications of two different matching techniques are compared, one is a popular method proposed by Hird et al. (1992) and the second is a less known method proposed by Lin et al. (2000). Considering the parameters presented in Table 3, the equivalent permeability with the matching technique proposed by Lin et al. (2000) is obtained as $k_{pl} = 0.012k_h$, which is a value very close to the one obtained with the formulation of Hird et al. (1992).

Comparing the long-term settlement plots of the two sides of the embankment studied in this paper (Fig. 9a) the numerical results obtained using the two matching techniques are very similar. Also in terms of lateral deformations, the difference between the results corresponding to the application of two matching techniques is not noticeable (Fig. 9b). It is difficult to point out which is the more appropriate matching technique as the results are almost identical.

Geotextiles and Geomembranes. Submitted 13 November 2016; accepted 2 July 2017.
http://dx.doi.org/10.1016/j.geotexmem.2017.07.004

When adopting the combined matching technique of Hird et al. (1992), one has to preselect the value of the width of the equivalent plane-strain unit cell in order to obtain the corresponding permeability, as the model takes into account both geometry and permeability factors. By changing the value of B, in this instance for example adopting $B = 1$, the permeability value changes accordingly ($k_{pl} = 0.0504k_h$). It is observed that greater spacing between the drains leads to a remarkable increase in settlement predictions (Fig. 10a). Distribution of the effective stress parameter is slightly influenced by increase in drain spacing, resulting in lower decrease/increase of stresses within the PVD improved soil (Fig. 10b). Variations of the state parameters e and χ are also decreased with increase in drain spacing (Figs. 10c and d). In fact, higher values of equivalent plane-strain permeabilities obtained from using higher drain spacing leads to a higher rate of consolidation and consequently higher degradation of the inter-particle bonds (destructuration) within the PVD improved area. The recovery in between the drains does not reach the values of the simulation with $B = 0.5$. An advantage of assuming a greater value of B is the possibility to better control the FE mesh, adopting a less refined mesh, therefore increasing the efficiency of the simulation.

As in the formulation of the equivalent plane-strain permeability proposed by Lin et al. (2000) the geometry of the model is not considered, adopting different values for the equivalent plane-strain cell does not alter the predictions. This implies that no further simplification of the numerical model is feasible when the matching technique of Lin et al. (2000) is used. Therefore, adopting an equivalent plane-strain width ($2B$) equal to the drain spacing (S) is necessary for modeling PVD improved soil foundations.

4 Conclusions

In this paper, the influence of PVD installation on the consolidation response of the soft soils was analyzed. A case study test embankment, namely Haarajoki embankment, was numerically simulated using three different soil models (MCC, S-CLAY1S and the newly developed Creep-SCLAY1S) in order to highlight the importance of considering time-effects

(i.e., creep) in modeling natural soil behavior at practical level. Based on the results, the following conclusions can be drawn;

- Creep-SCLAY1S model is capable of providing reasonably accurate predictions of the delayed soft soil response in general, and the PVD installation effects in particular.
- As time-independent models such as MCC are not able to reproduce the delayed response of the soil, they should not be used for modeling case studies where the soil response is considerably prone to creep.
- Where test data is not available, the adopted method to estimate the intrinsic creep index values (i.e., $C_{\alpha i} = C_{\alpha}\lambda_i/\lambda$) is reasonably reliable for practical applications.
- The installation of PVDs significantly accelerates the settlement of soft clays and the process of excess pore pressure dissipation. Hence with their application, a construction project can proceed faster and safer, without further damaging settlements in subsequent years.
- The presence of vertical drains alters the stress field and the soil state parameters, leading to further densification of the soil and a higher effective stress level in the PVD improved area.
- An appropriate matching technique to convert the 3D vertical drain system into equivalent plane-strain condition allows using a representative 2D plane-strain model, which is computationally less expensive. Application of the two different matching techniques, proposed by Hird et al. (1992) and Lin et al. (2000), led to fairly similar results. Nevertheless, the matching technique proposed by Hird et al. (1992) appears to be more versatile as it takes into account both geometry and permeability aspects, and as such its application allows to better control the efficiency of the numerical simulation.

References

Abuel-Naga, H.M., Bergado, D.T., Gniel, J., 2015. Design chart for prefabricated vertical drains improved ground. Geotext. Geomemb. 43, 537–546.

Geotextiles and Geomembranes. Submitted 13 November 2016; accepted 2 July 2017.
http://dx.doi.org/10.1016/j.geotexmem.2017.07.004

Berry, P. L., and Poskitt, T. J., 1972. The consolidation of peat. Géotechnique 22 (1), 27-52.

Brinkgreve R.B.J., Engin E., Swolfs W.M., 2014. Plaxis 2014 reference manual, Plaxis, Delft, Netherlands.

Cascone, E., Biondi, G., 2013. A case study on soil settlements induced by preloading and vertical drains. Geotext. Geomemb. 38, 51–67.

Chen, J.F., Tolooiyan, A., Xue, J.F., Shi, Z.M., 2016. Performance of a geogrid reinforced soil wall on PVD drained multilayer soft soils. Geotext. Geomemb. 44 (3), 219–229.

Deng, Y.B., Xie, K.H., Lu, M.M., Tao, H.B., Liu, G.B., 2013. Consolidation by prefabricated vertical drains considering the time dependent well resistance. Geotext. Geomemb. 36, 20–26.

Finnish National Road Administration, 1997. Competition to calculate settlements at the Haarajoki test embankment. Competition programme, competition materials, Finnra, Helsinki, Finland.

Grimstad, G., Abate, S., Nordal, S., Karstunen, M., 2010. Modeling creep and rate effects in structured anisotropic soft clays. Acta Geotechnica 5, 69–81.

Hansbo, S., 1979. Consolidation of clay by band-shaped vertical drains. Ground Eng. 12 (5), 16–25.

Hird C.C., Pyrah I.C., Russell D., 1992. Finite element modeling of vertical drains beneath embankments on soft ground. Géotechnique 42 (3). 499–511.

Hu, Y.Y., Zhou, W.H., Cai, Y.Q., 2014. Large-strain elastic viscoplastic consolidation analysis of very soft clay layers with vertical drains under preloading. Can. Geotech. J. 51, 144–157.

Indraratna, B., Sathananthan, I., Rujikiatkamjorn, C., Balasubramaniam A. S., 2005. Analytical and numerical modelling of soft soil stabilized by PVD incorporating vacuum preloading. Int. J. Geomech. 5 (2), 114–124.

Karstunen, M., Krenn, H., Wheeler, S. J., Koskinen, M., Zentar, R., 2005. The effect of anisotropy and destructuration on the behaviour of Murro test embankment. Int. J. Geomech. 5 (2), 87–97.

Karstunen, M., Rezania, M., Sivasithamparam, N., Yin, Z-Y., 2015. Comparison of anisotropic rate-dependent models for modeling consolidation of soft clays. Int. J. Geomech. 15 (5), 1–11.

Kim, Y.T., 2012. Strain rate-dependent consolidation behaviors of embankment with or without vertical drains. Marine Georesour. Geotech. 30 (4), 274–290.

Kim, Y.T., Lee, S.R., 1997. An equivalent model and back-analysis technique for modelling in situ consolidation behavior of drainage-installed soft deposits. Comp. Geotech. 20 (2), 125–142.

Lam, L.G., Bergado, D.T., Hino, T., 2015. PVD improvement of soft Bangkok Clay with and without vacuum preloading using analytical and numerical analyses. Geotext. Geomemb. 43, 547–557.

Leoni, M., Karstunen, M., and Vermeer, P.A., 2008. Anisotropic creep model for soft soils. Géotechnique 58 (3), 215–226.

Lin D.G., Kim H.K., Balasubramaniam A.S., 2000. Numerical modelling of prefabricated vertical drain. Geotech. Eng. J. of SEAGS 31 (2), 109–125.

Lo, S.R., Karim, M.R., Gnanendran, C.T., 2013. Consolidation and creep settlement of embankment on soft clay: prediction versus observation. In: Geotechnical Predictions and Practice in Dealing with Geohazards. Springer Netherlands, 77–94.

Mesri, G., Godlewski, P.M., 1977. Time and stress-compressibility interrelationship. J. Geotech. Eng-ASCE 103 (5), 417–430.

Nguyen, T.T., Indraratna, B., 2017. Experimental and numerical investigations into hydraulic behaviour of coir fibre drain. Can. Geotech. J. 54 (1), 75-87

Rezania, M., Sivasithamparam, N., and Mousavi-Nezhad, M., 2014. On the stress update algorithm of an advanced critical state elasto-plastic model and the effect of yield function equation. Finite Elem. Anal. Des. 90, 74-83.

Rezania, M., Taiebat, M. and Poletti, E., 2016. A viscoplastic SANICLAY model for natural soft soils. Comp. Geotech. 73, 128-141.

Rezania, M., Mousavi-Nezhad, M., Zanganeh, H., Castro, J., Sivasithamparam, N., 2017. Modelling pile setup in natural clay deposit considering soil anisotropy, structure, and creep effects: Case study. Int. J. Geomech. 04016075, 1–13.

Roscoe, K.H., Burland, J.B., 1968. On the generalized stress-strain behaviour of 'wet' clay. Engineering plasticity, Cambridge University Press, Cambridge, U.K. 553–609.

Rowe, R.K., Taechakumthorn, C., 2008. Combined effect of PVDs and reinforcement on embankments over rate-sensitive soils. Geotext. Geomemb. 26, 239–249.

Wheeler, S.J., Näätänen, A., Karstunen, M., Lojander, M., 2003. An anisotropic elastoplastic model for soft clays. Can. Geotech. J. 40, 403–418.

Sivasithamparam, N., Karstunen M., Bonnier, P., 2015. Modelling creep behaviour of anisotropic soft soils. Comp. Geotech. 69, 46–57.

Wang, J., Cai, Y. Ma, J., Chu, J., Fu, H., Wang, P., Jin, Y., 2016. Improved vacuum preloading method for consolidation of dredged clay-slurry fill. J. Geotech. Geoenviron. Eng. 06016012, 1–5.

Xiao, D.P., 2001. Consolidation of soft clay using vertical drains. Ph.D. Thesis, Nanyang Technological University, Singapore.

Xue, J-F., Chen, J-F., Liu, J-X. , Shi, Z-M., 2014. Instability of a geogrid reinforced soil wall on thick soft Shanghai clay with prefabricated vertical drains: A case study. Geotext. Geomemb. 42, 302–311.

Yildiz, A., 2009. Numerical analyses of embankments on PVD improved soft clay. Adv. Eng. Softw. 1047–1055.

Yildiz, A., Karstunen, M., and Krenn, H., 2009. Effect of anisotropy and destructuration on behaviour of Haarojoki test embankment. Int. J. Geomech. 153–165.

Zhu, G. and Yin, J.H., 2000. Finite element consolidation analysis of soils with vertical drain. Int. J. Numer. Anal. Met. 24 (4), 337–366.

Geotextiles and Geomembranes. Submitted 13 November 2016; accepted 2 July 2017.
http://dx.doi.org/10.1016/j.geotexmem.2017.07.004

List of notations

B	Half width of plane-strain unit cell	α_0	Initial value of anisotropy
c'	Cohesion	α	Scalar value of anisotropy
c_k	Permeability change index	β	Creep exponent
c_α	Creep index	χ	Bonding parameter
$c_{\alpha i}$	Intrinsic creep index	χ_0	Initial value of bonding parameter
D	Equivalent diameter of unit cell	γ	Unit weight
D_m	Equivalent diameter of mandrel	κ	Slope of swelling/recompression line from $e - lnp_0$diagram
D_s	Equivalent diameter of smear zone	κ^*	Modified slope of swelling/recompression line from $e - lnp_0$diagram
D_w	Equivalent diameter of drain	λ	Slope of post yield compression line from $e - lnp_0$diagram
E	Young's modulus	λ_i	Slope of intrinsic post yield compression line from $e - lnp_0$diagram
e_0	Initial void ratio	λ^*	Modified slope of post yield compression line from $e - lnp_0$diagram
e	Void ratio	λ_i^*	Modified slope of intrinsic post yield compression line from $e - lnp_0$diagram
K_0	coefficient of lateral earth pressure at rest	μ^*	Modified creep index
k	Permeability	μ_i^*	Intrinsic modified creep index
k_h	Horizontal permeability of undisturbed soil	ω	Rate of rotation
k_{hpl}	Equivalent plane-strain horizontal permeability	ω_d	Rate of rotation due to deviator stress
k_s	Horizontal permeability of smear zone	ζ	Parameter controlling absolute rate of destructuration
k_v	Vertical permeability of undisturbed soil	ζ_d	Parameter controlling relative effectiveness of destructuration rate
M	Stress ratio at critical state	ν	Poisson's coefficient
R	Equivalent radius of unit cell	ϕ'	Friction angle
R_s	Equivalent radius of smear zone	τ	Reference time
R_w	Equivalent radius of drain	NCS	Normal consolidation surface
S	Drain spacing	POP	Pre-overburden pressure

Geotextiles and Geomembranes. Submitted 13 November 2016; accepted 2 July 2017.
http://dx.doi.org/10.1016/j.geotexmem.2017.07.004

Table 1 – Model constants adopted for Haarajoki clay layers

Type	Parameter	Layer 1a (0-1m)	Layer 1b (1-2m)	Layer 2 (2-6m)	Layer 3 (6-7m)	Layer 4 (7-12m)	Layer 5 (12-15m)	Layer 6 (15-18m)	Layer 7 (18-22.2m)
Initial stress state	e_0	1.25	1.25	2.90	2.60	2.35	2.20	2.00	1.25
	γ (kN/m^3)	17.5	17.5	14.3	14.3	15.1	15.1	15.7	17.5
	POP (kN/m^2)	110	32	32	32	32	32	32	32
Elasticity	ν	0.2	0.2	0.2	0.2	0.2	0.2	0.2	0.2
	κ	--------	0.010	0.010	0.030	0.036	0.030	0.034	0.004
Critical State	M	--------	1.60	1.15	1.43	1.15	1.20	1.55	1.55
	λ	--------	0.20	1.33	0.96	0.96	1.06	0.45	0.10
	λ_i	--------	0.20	0.38	0.27	0.26	0.30	0.13	0.03
Anisotropy*	α_0	--------	0.63	0.44	0.55	0.44	0.46	0.61	0.61
	ω	--------	37	33	49	44	35	36	37
	ω_d	--------	1.02	0.70	0.97	0.70	0.76	1.01	1.01
Destructuration**	χ_0	--------	4	22	30	45	45	45	45
	ζ	--------	8	8	8	8	8	8	8
	ζ_d	--------	0.2	0.2	0.2	0.2	0.2	0.2	0.2
Viscosity	μ^*	--------	1.16E-3	4.44E-3	3.47E-3	3.73E-3	4.32E-3	1.95E-3	5.79E-3
Permeability	k_h (m/d)	3.46E-4	3.46E-4	1.04E-4	8.64E-5	8.64E-5	8.64E-5	8.64E-5	3.46E-4
	k_v (m/d)	1.73E-4	1.73E-4	5.18E-5	4.32E-5	4.32E-5	4.32E-5	4.32E-5	1.73E-4
	c_k	0.45	0.45	1.12	1.29	0.74	0.61	0.40	0.40

*calculated based on the method proposed by Wheeler et al., 2003
**calculated based on the method proposed by Karstunen et al., 2005

Table 2 – Parameters adopted for matching technique

S [m]	B [m]	R [m]	R_s [m]	R_w [m]	R_s/R_w	k_h/k_s
1	0.5	0.564	0.268	0.034	8	20

Table 3 – Modified coefficients of permeability according to the matching techniques

Layer	Layer 1a (0-1m)	Layer 1b (1-2m)	Layer 2 (2-6m)	Layer 3 (6-7m)	Layer 4 (7-12m)	Layer 5 (12-15m)	Layer 6 (15-18m)	Layer 7 (18-22.2m)
k_{hpl} (Hird et al., 1992)	4.36E-6	1.31E-6	1.09E-6	1.09E-6	1.09E-6	1.09E-6	1.09E-6	4.36E-6
k_{hpl} (Lin et al., 2000)	4.15E-6	1.25E-6	1.04E-6	1.04E-6	1.04E-6	1.04E-6	1.04E-6	4.15E-6

Geotextiles and Geomembranes. Submitted 13 November 2016; accepted 2 July 2017.
http://dx.doi.org/10.1016/j.geotexmem.2017.07.004

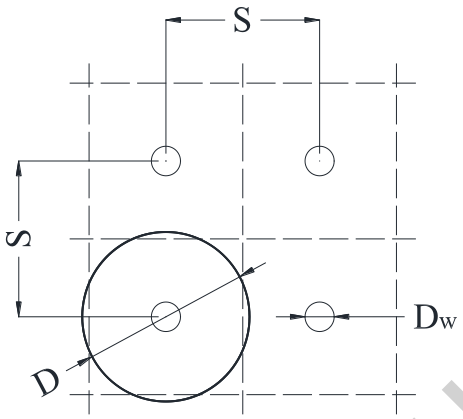

(a)

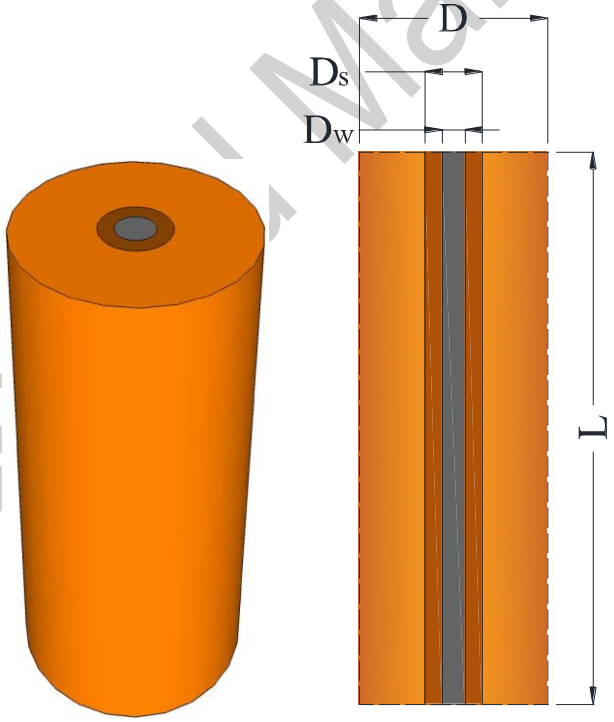

(b)

Fig. 1. PVD pattern: (a) square pattern; (b) drain with smear zone

Geotextiles and Geomembranes. Submitted 13 November 2016; accepted 2 July 2017.
http://dx.doi.org/10.1016/j.geotexmem.2017.07.004

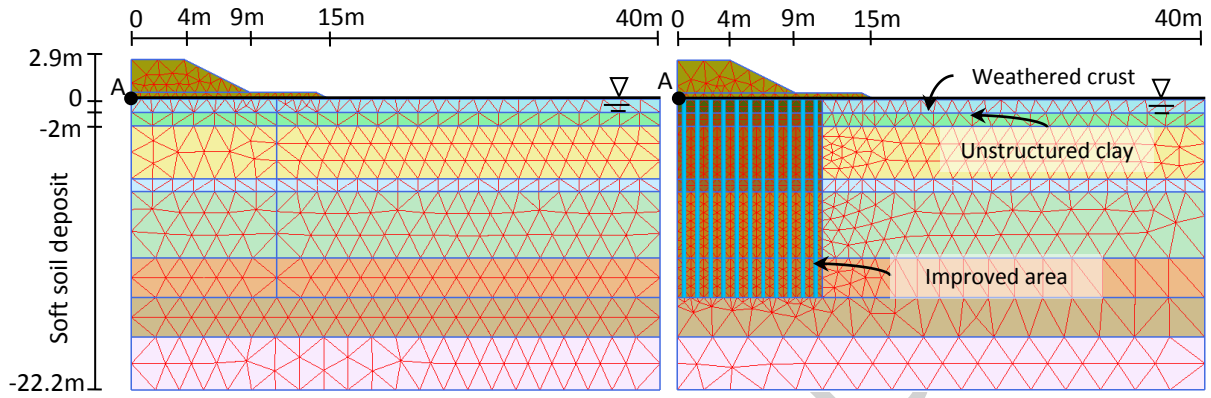

Fig. 2. Geometry of the finite element models adopted for the simulation of Haarajoki test embankment and the position of PVDs; Left: unimproved side; Right: improved side of the foundation soil

Geotextiles and Geomembranes. Submitted 13 November 2016; accepted 2 July 2017.
http://dx.doi.org/10.1016/j.geotexmem.2017.07.004

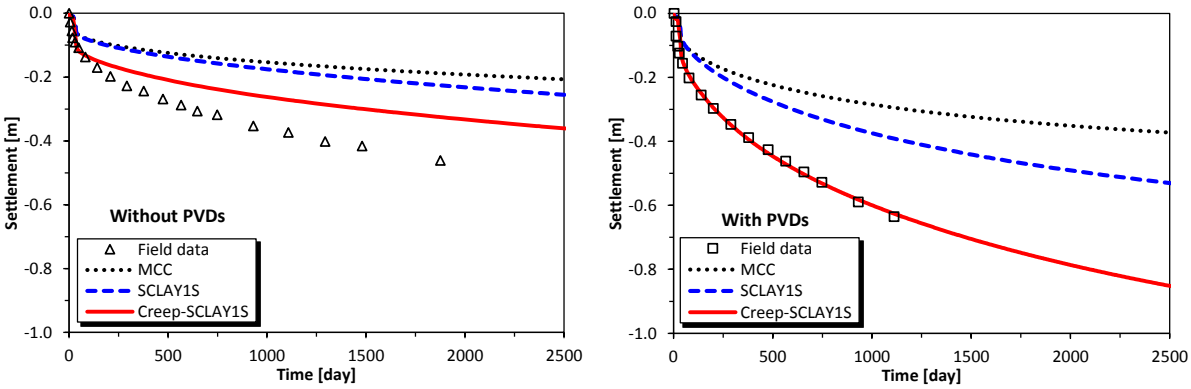

(a) (b)

Fig. 3. Time- settlements plots for Haarajoki embankment at centreline: (a) without PVDs; (b) with PVDs

Geotextiles and Geomembranes. Submitted 13 November 2016; accepted 2 July 2017.
http://dx.doi.org/10.1016/j.geotexmem.2017.07.004

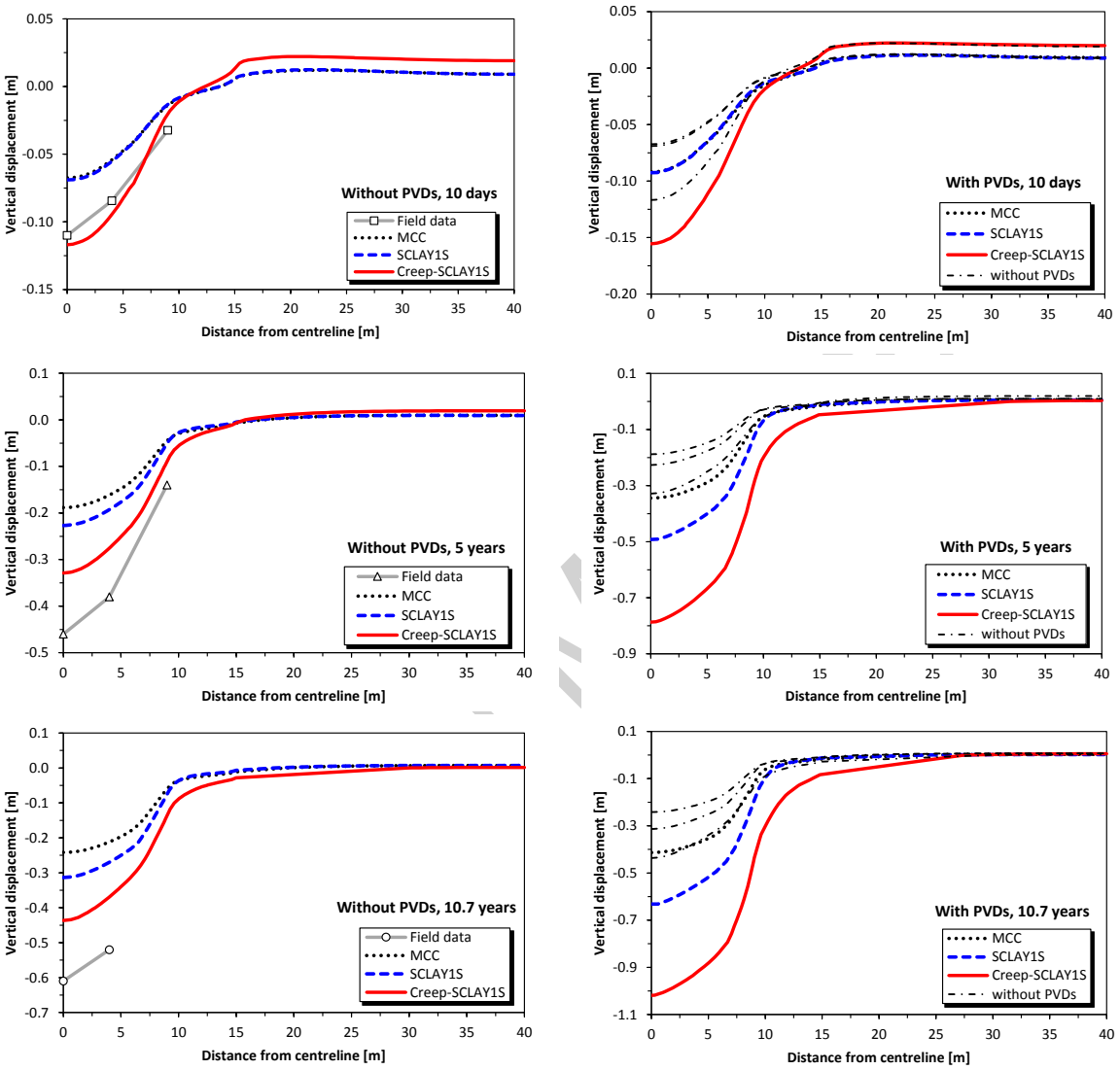

(a) (b)

Fig. 4. Surface settlement throughs for Haarajoki embankment: (a) without PVDs; (b) with PVDs

Geotextiles and Geomembranes. Submitted 13 November 2016; accepted 2 July 2017.
http://dx.doi.org/10.1016/j.geotexmem.2017.07.004

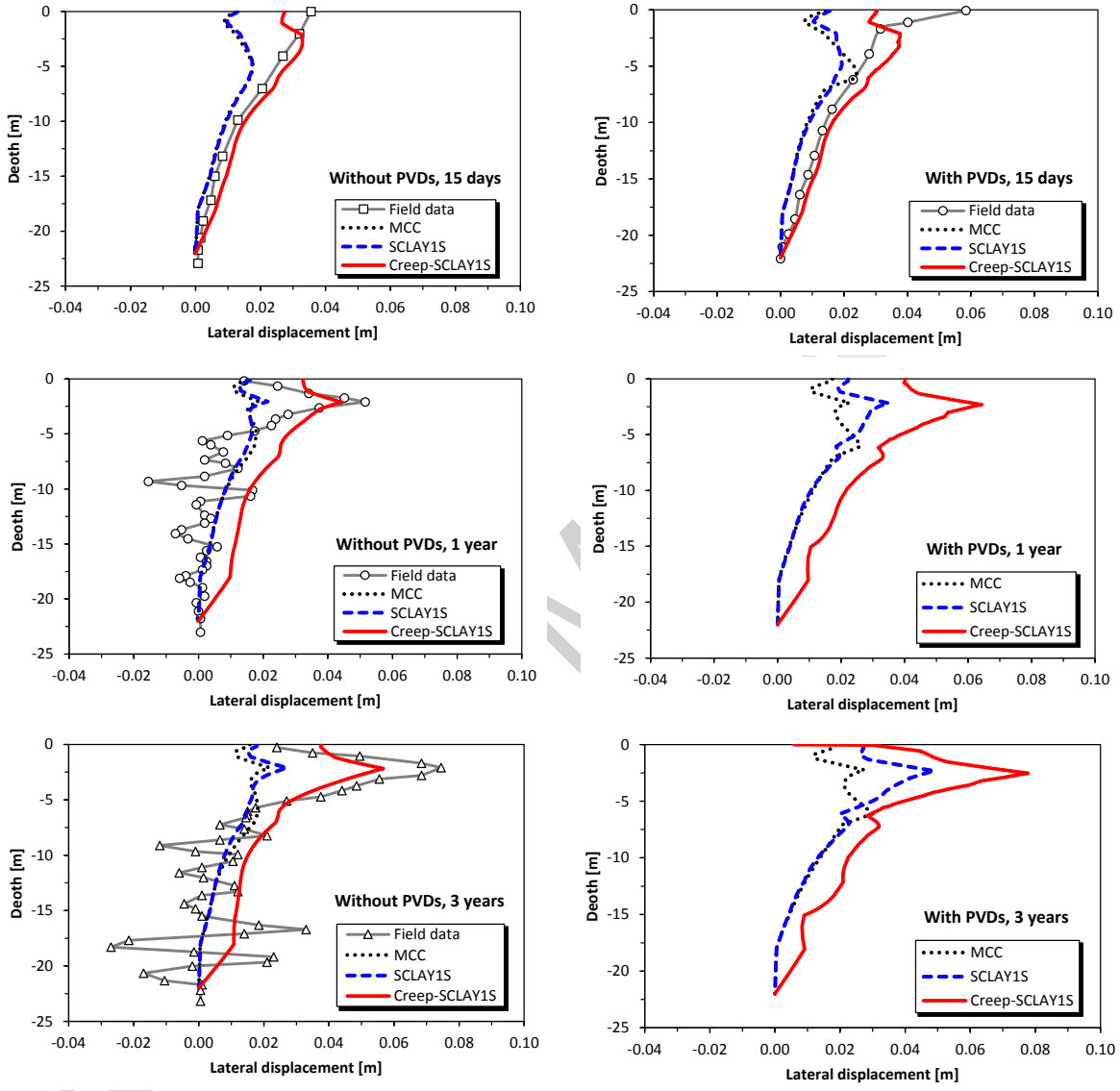

Fig. 5. Lateral displacement predictions for Haarajoki embankment under the crest: (a) without PVDs (b) with PVDs

Geotextiles and Geomembranes. Submitted 13 November 2016; accepted 2 July 2017.
http://dx.doi.org/10.1016/j.geotexmem.2017.07.004

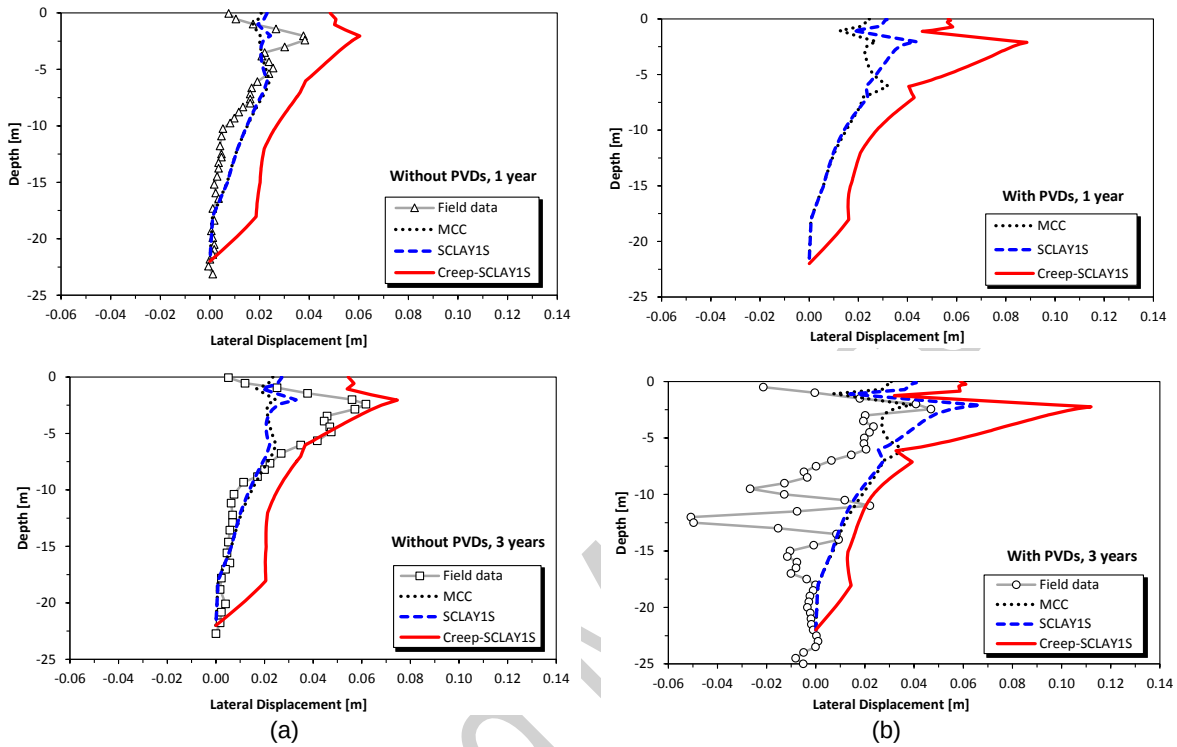

Fig. 6. Lateral displacements predictions for Haarajoki embankment under the toe: (a) without PVDs; (b) with PVDs

Geotextiles and Geomembranes. Submitted 13 November 2016; accepted 2 July 2017.
http://dx.doi.org/10.1016/j.geotexmem.2017.07.004

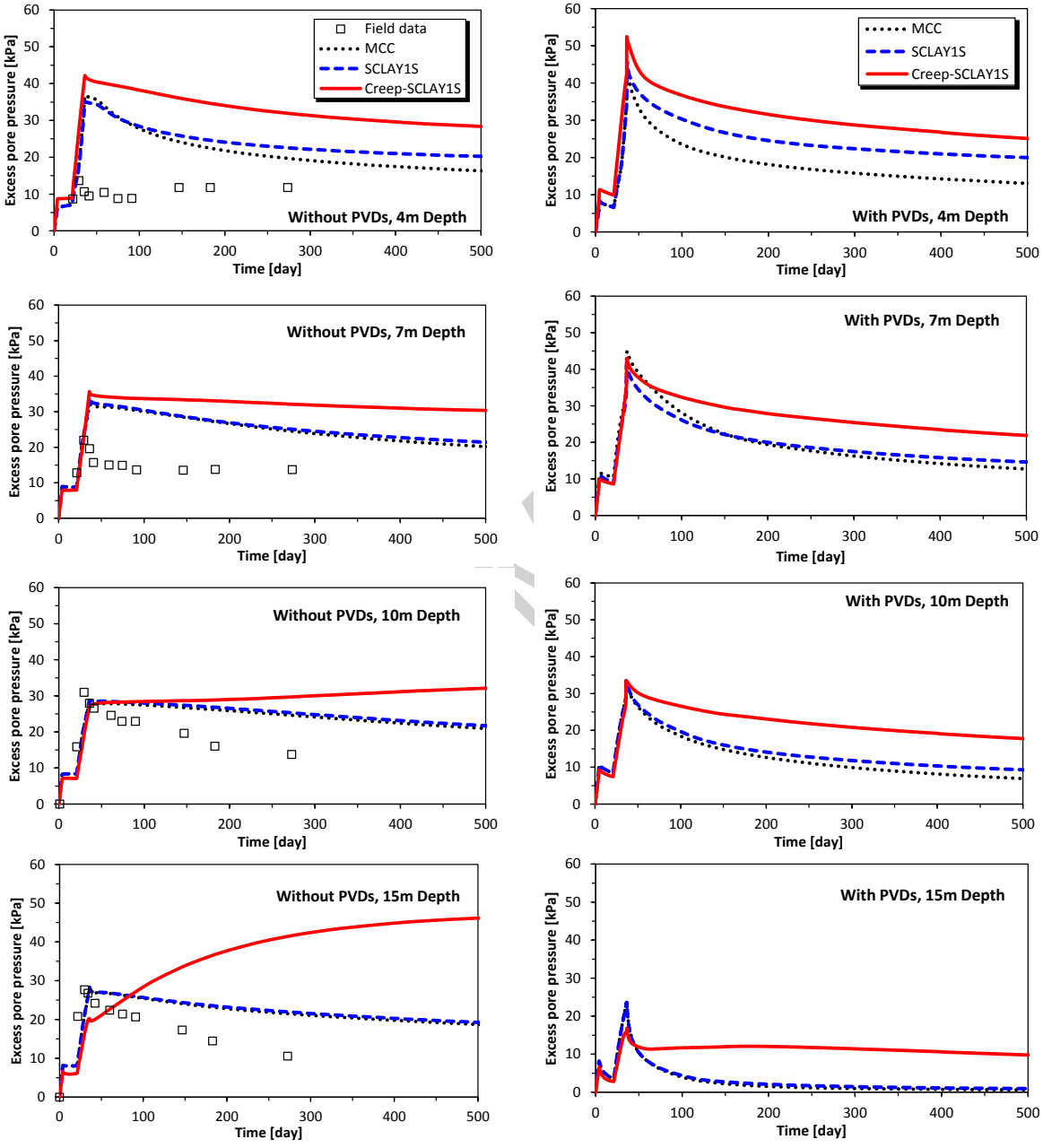

Fig. 7. Excess pore water pressure dissipation with time at different depths: (a) without PVDs; (b) with PVDs

Geotextiles and Geomembranes. Submitted 13 November 2016; accepted 2 July 2017.
http://dx.doi.org/10.1016/j.geotexmem.2017.07.004

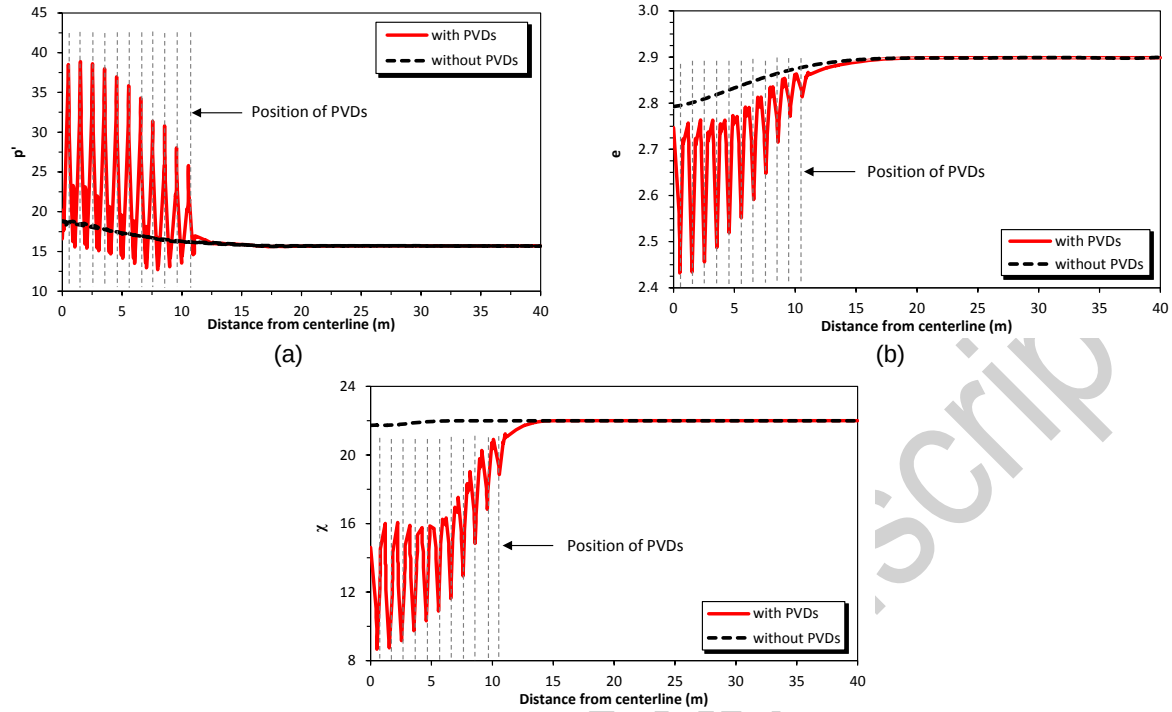

Fig. 8. Effect of installation of vertical drains: (a) mean effective stress distribution 15 days after construction; (b) void ratio distribution 1 year after construction; (c) bonding parameter distribution 1 year after construction

Geotextiles and Geomembranes. Submitted 13 November 2016; accepted 2 July 2017.
http://dx.doi.org/10.1016/j.geotexmem.2017.07.004

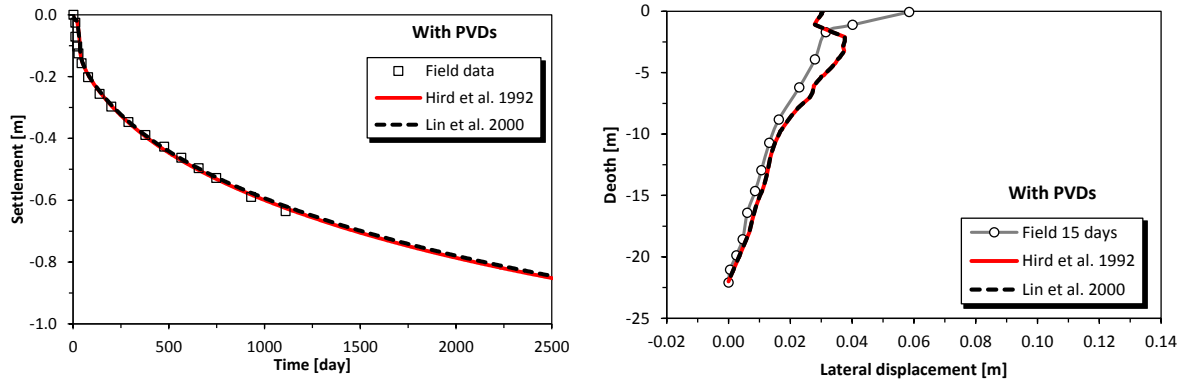

(a) (b)

Fig. 9. Comparison of matching techniques: (a) settlements at centerline; (b) lateral displacements under the crest

Geotextiles and Geomembranes. Submitted 13 November 2016; accepted 2 July 2017.
http://dx.doi.org/10.1016/j.geotexmem.2017.07.004

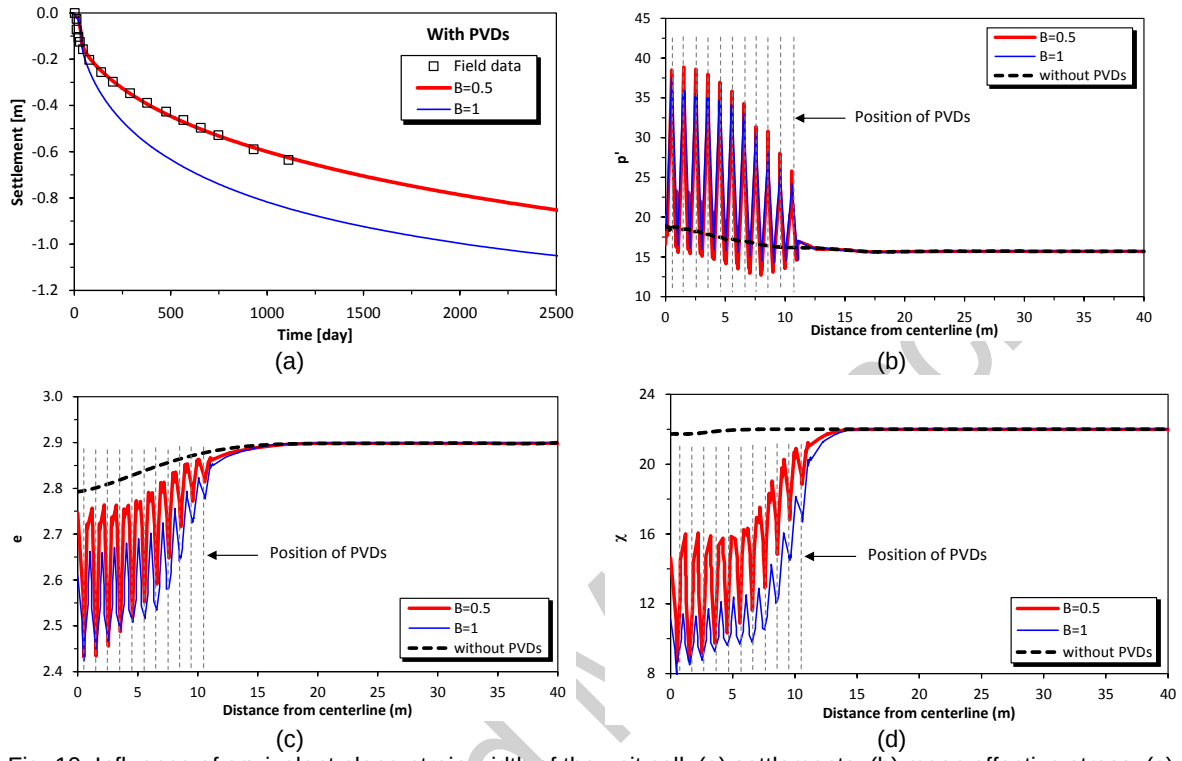

Fig. 10. Influence of equivalent plane-strain width of the unit cell: (a) settlements; (b) mean effective stress; (c) void ratio; (d) bonding parameter